Capacity of prestressed concrete bridge decks under fatigue loading

Lantsoght, Eva O.L.; van der Veen, Cor; Koekkoek, Rutger; Sliedrecht, Henk

DOI
10.2749/ghent.2021.0313

Publication date
2021

Document Version
Accepted author manuscript

Citation (APA)
Lantsoght, E. O. L., van der Veen, C., Koekkoek, R., & Sliedrecht, H. (2021). *Capacity of prestressed concrete bridge decks under fatigue loading*. 313-321. Paper presented at IABSE Congress, Ghent 2021: Structural Engineering for Future Societal Needs, Ghent, Virtual, Belgium. https://doi.org/10.2749/ghent.2021.0313

Capacity of prestressed concrete bridge decks under fatigue loading

Eva O.L. Lantsoght

Universidad San Francisco de Quito, Quito, Ecuador

Delft University of Technology, Delft, the Netherlands

Cor van der Veen

Delft University of Technology, Delft, the Netherlands

Rutger Koekkoek

BAM, Gouda, the Netherlands

Henk Sliedrecht

Rijkswaterstaat, Utrecht, the Netherlands

Contact: e.o.l.lantsoght@tudelft.nl

Abstract

In the Netherlands, existing slab-between-girder bridges with prestressed girders and thin transversely prestressed concrete decks require assessment. The punching capacity was studied in a previous series of experiments, showing a higher capacity thanks to compressive membrane action in the deck. Then, concerns were raised with regard to fatigue loading. To address this, two series of large-scale experiments were carried out, varying the number of loads (single wheel print versus double wheel print), the loading sequence (constant amplitude versus variable amplitude, and different loading sequences for variable amplitude), and the distance between the prestressing ducts. An S-N curve is developed for the assessment of slab-between-girder bridges. The experiments showed that compressive membrane actions enhances the capacity of thin transversely prestressed decks subjected to fatigue loading.

Keywords: Assessment, Fatigue, Live loads, Punching shear, Shear, Slab-between-girder bridges.

1 Introduction

The Dutch bridges from the decades following the Second World War were designed for the live loads of that era, which were lower than the currently code-prescribed live loads. At the same time, the previously used national codes in The Netherlands, such as NEN 6720:1995 [1] contained provisions that resulted in larger calculated shear and punching shear capacities than when using NEN-EN 1992-1-1:2005 [2]. As a result, an analytical assessment of existing concrete bridges often results in the conclusion that the shear or punching shear capacity is insufficient [3]. One bridge type that upon assessment is often found to be insufficient for punching shear is the slab-between-girder bridge. These bridges consist of prestressed girders and thin transversely prestressed concrete decks that are cast between the prestressed girders. In total, about 70 of these structures are present in the Dutch road network [4].

When the punching shear capacity of the thin transversely prestressed concrete decks is determined with the Eurocode provisions [2], the capacity-enhancing effect of compressive membrane action [5-7] is not taken into account. To study the enhancement from compressive membrane action on the ultimate capacity of the thin transversely prestressed decks in slab-between-girder bridges, static tests on a half-scale slab-between-girder bridge built in the Stevin II Laboratory of Delft University of Technology were carried out [4, 8]. These experiments showed that the deck fails in punching shear, whereas it was designed to fail in flexure, and that its ultimate capacity is on average 2.3 times larger than the Eurocode punching shear capacity [2]. The result of these static tests improved the assessment of the existing slab-between-girder bridges in The Netherlands.

Under fatigue loading, progressive cracking and increases in strains occur. Fatigue tests on partially prestressed concrete beams [9-12] showed that the failure mode can change from flexural failure to a brittle shear failure. Therefore, there were concerns about the preservation of the capacity-enhancing effect of compressive membrane action under fatigue loading. This paper reports two series of experiments on this topic.

2 Description of experiments

2.1 Test setup

Two series of experiments were carried out. In the first series, the same test setup was used as for the static tests (4 girders with 3 decks cast in between). Afterwards, the decks that were tested for the static tests were removed, and a new deck was cast between the existing girders for the middle panel. Figure 1a and b show the geometry of the specimen for the first series. The overall dimensions of the specimen for the first series is 6.4 m by 12 m. The precast girders are 10.95 m long and 1.3 m high, and placed at a centre-to-centre spacing of 1.8 m. The slab is 100 mm thick and 1050 mm wide. The transverse prestressing is applied by post-tensioning of tendons in ducts spaced 400 mm apart. In total, 30 ducts with a diameter of 40 mm are cast in the slab. One part of the new deck had a duct diameter of 30 mm and spacing of 300 mm. The crossbeams are 810 mm × 350 mm, and cast and post-tensioned in the laboratory.

The second series used a new model bridge, with three girders and two decks. For the second series, both the top flange of the girders and the decks were cast in the laboratory. Figure 1c and d show the specimen for the second series. The overall dimensions of the specimen are 4.6 m by 12 m. All details of the experiments are given in the background report [13-15].

A steel frame with a hydraulic jack is used to apply the load to the specimen. The loading plate size for the original deck of specimen 1 is 200 mm × 200 mm, which is 1:2 scale of the wheel print from NEN EN 1991-2:2003 [16]. For the new deck, the loading plate is 115 mm × 150 mm, which is 1:2 scale of the wheel print used in The Netherlands for fatigue assessment of bridge joints. A layer of 10 mm of rubber is placed between the steel plate and deck to avoid stress concentrations.

2.2 Materials

The concrete compressive strength is determined on cube specimens cast together with the specimens and stored in the fog room of the laboratory. An overview of the properties is given in Table 1, which shows that the concrete compressive strength of the specimen used in the second series of tests is on average 7% larger than the compressive strength of the specimen from the first series of tests.

The mild steel used in the girders in specimen 1 is B500A for the bars with a diameter of 6 mm and smaller (B500B is not commercially available for these bar diameters), and B500B for the larger bars. In existing bridges, B500B is used for all mild steel. The mild steel in the deck of specimen 1 consists of diameter 6 mm longitudinal bars top and bottom at 200 mm on centre and diameter 6 mm transverse bars top and bottom at 250 mm on centre. In specimen 2, the mild steel in the deck consist of diameter 8 mm longitudinal bars top and bottom at 240 mm on centre in the long span direction and at 200 mm on centre in the short span direction. Table 2 gives the strength properties (f_{ym} for the average yield strength and

f_{tm} for the average tensile strength) of the mild steel for the different bar diameters (φ) used in these experiments.

Table 1. Overview of material properties

Specimen nr	Element	$f_{cm,cube}$ (MPa)	Age (days)
1	Girders	90	273
1	Slab (original)	75	28
1	Crossbeams	71	28
1	Slab (newly cast)	68	28
1	Slab (newly cast)	77	56
1	Slab (newly cast)	78	188
2	Crossbeams	78	149
2	Slab + top flange, cast 1	81	28
2	Slab + top flange, cast 2	79	28

Table 2. Properties (yield strength fym and tensile strength ftm) of mild steel as measured on samples.

φ (mm)	f_{ym} (MPa)	f_{tm} (MPa)	φ (mm)
6	525	580	6
8	552	641	8
10	516	625	10
12	527	623	12
16	517	612	16

The clear cover is 7 mm. For both specimens 1 and 2, the prestressing steel used in the girders is Y1860S and consists of tendons. The prestressing steel of the slab and crossbeam is Y1100H and consists of prestressing bars. The diameter of the prestressing bars in the deck is 15 mm, and for the fatigue tests an average compression force from the transverse prestressing of 2.5 MPa is applied.

2.3 Loading method

The static tests were carried out with a stepwise increasing loading protocol, see Figure 2a. The load step for the lower load levels (up to 100 kN) was 25 kN, and for the higher load levels the load step was 50 kN. When the load is constant, the test engineers inspect the specimen and mark the cracks. In the first series of experiments, two experiments were carried out with a limited number of cycles at increasing load levels (three cycles per load level), see Figure 2b. These experiments and the static tests were carried out in a displacement-controlled way. Then, for the fatigue tests, the number of cycles to failure was determined for loading between a predetermined upper limit and a lower limit which is 10% of the load of the upper limit. The load is applied as a sine function with a frequency of 1 Hz, see Figure 2c. If failure did not occur after a large number of cycles for a predetermined load level, then a higher load level was applied until failure occurred. The fatigue tests were carried out in a force-controlled way.

3 Results

3.1 Overview of test results

For the experiments on the first specimens, the tests are numbered consecutively as BBX, with X the number of the test and BB the abbreviation for Brienenoord Bridge, the bridge after which the setup was modelled. The results of the 19 static tests from the first series are reported in [4]. Two tests with a limited number of cycles with the loading protocol from Figure 2b (BB17 and BB18) were carried out on the first specimen, two fatigue tests were carried out on the original setup (BB23 and BB24), and five additional fatigue tests (BB26, BB28, BB29, BB30, BB32) were carried out on the new deck.

For the second series of experiments, the test number consists of the name of the series FAT (fatigue tests), the number of the experiment, S (static test) or D (dynamic test), and 1 (single wheel print) or 2 (double wheel print). In the second series, a total of 13 experiments (3 static and 10 dynamic) were carried out. Experiments FAT2D1 and FAT3D1 are used for comparison to BB32 to confirm that the second specimen

behaves in a similar way as the first specimen, and that the results can thus be analysed together.

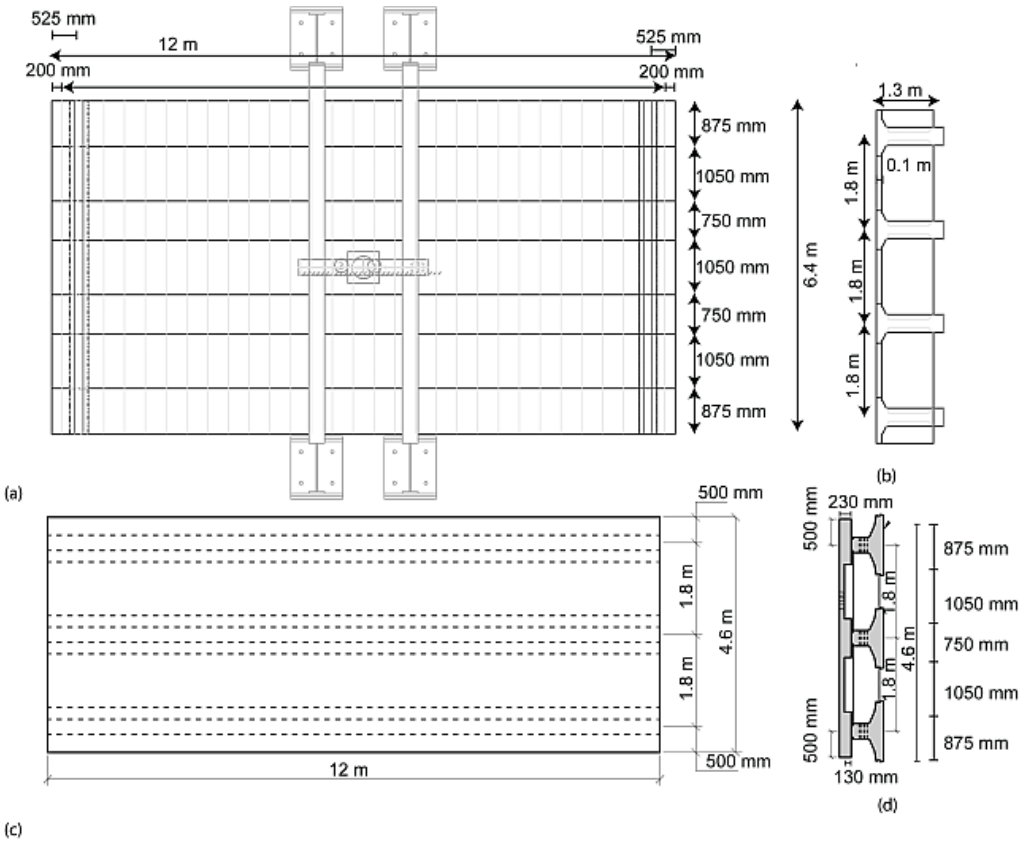

Figure 1. Test setup for fatigue experiments: (a) top view of first series, showing four girders and three decks; (b) section of specimen of first series; (c) top view of second series, showing three girders and two decks; (d) section of specimen of second series.

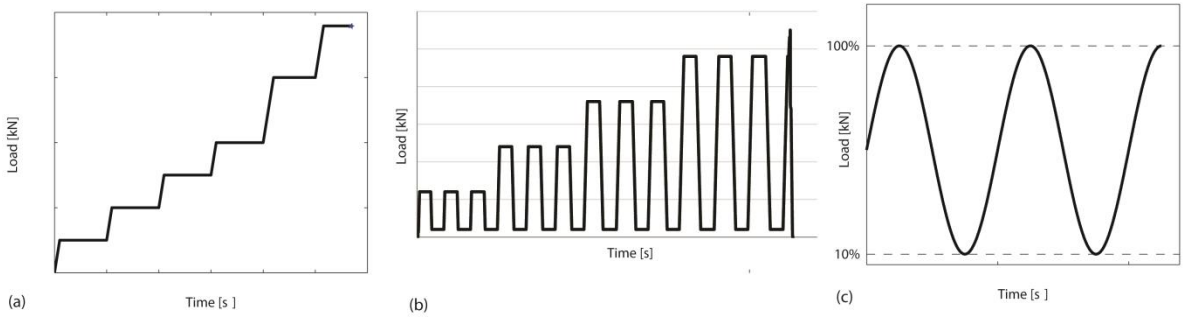

Figure 2. Loading protocol used in the experiments: (a) stepwise monotonically increasing loading protocol for static testing; (b) three load cycles per load level for tests with limited number of cycles; (c) loading applied during fatigue tests (excerpt of 5 seconds from loading protocol).

Table 3. Overview of punching fatigue experiments

Experiment	Spec	Size load (mm × mm)	Wheel	ϕ_{duct} (mm)	F (kN)	F/P_{max}	N	Age (days)	$f_{cm,cube}$ (MPa)
BB17	1	200 × 200	S	40	275	0.80	13	147	82.6
BB18	1	200 × 200	S	40	291	0.85	16	56	82.6
BB23	1	200 × 200	S	40	200	0.60	24,800	301	79.9
BB24	1	200 × 200	S	40	150	0.45	1,500,000	307-326	79.9
BB26	1, new	150 × 115	S	30	165	0.48	1,405,337	35-59	70.5-76.7
BB28	1, new	150 × 115	S	40	165	0.48	1,500,000	68-97	76.8-77.1
					200	0.58	1,000,000	97-113	77.1-77.3
					240	0.70	7144	113	77.3
BB29	1, new	150 × 115	S	40	200	0.58	1,500,000	117-136	77.3-77.5
					220	0.64	264,840	136-139	77.5-77.6
BB30	1, new	150 × 115	D	40	280	0.58	100,000	143-144	77.6
					240	0.50	1,400,000	144-162	77.6-77.8
					280	0.58	750,000	162-171	77.8-77.9
					320	0.67	500,000	171-177	77.9-78.0
					360	0.75	32,643	177	78.0
BB32	1, new	150 × 115	S	40	240	0.70	10,000	184	78.1
					200	0.58	272,548	185-187	78.1
FAT2D1	2	150 × 115	S	40	240	0.69	100,000	102-144	82.6-84.6
					200	0.58	2,915,123		
					240	0.69	100,000		
					260	0.75	150,000		
					280	0.81	20,094		
FAT3D1	2	150 × 115	S	40	240	0.69	200,000	149-168	84.9-85.8
					200	0.58	1,000,000		

					240	0.69	100,000		
					260	0.75	300,000		
					280	0.81	6114		
FAT4D1	2	150 × 115	S	40	200	0.58	1,000,000	169-190	85.8-86.8
					240	0.69	200,000		
					260	0.75	100,000		
					280	0.81	63,473		
FAT5D1	2	150 × 115	S	40	280	0.71	10,000	192-217	91.6-89.6
					200	0.51	1,000,000		
					240	0.61	100,000		
					260	0.66	1,000,000		
					280	0.71	1424		
FAT6D1	2	150 × 115	S	40	280	0.71	10,000	219-239	89.6-88.8
					200	0.51	1,000,000		
					240	0.61	100,000		
					280	0.71	160,000		
					200	0.51	410,000		
					280	0.71	26,865		
FAT9D2	2	150 × 115	D	40	380	0.59	500,000	246-255	88.5-88.2
					420	0.65	209,800		
FAT10D2	2	150 × 115	D	40	360	0.63	100,000	260-284	90.2-91.3
					320	0.56	1,000,000		
					360	0.63	950,928		
FAT11D2	2	150 × 115	D	40	380	0.67	100,000	288-315	91.5-92.8
					340	0.60	1,000,000		
					380	0.67	1,100,000		
					420	0.75	1720		

FAT12D1	2	150 × 115	S	40	350	0.89	30	318	85.9
FAT13D1	2	150 × 115	S	40	340	0.86	38	319	85.8

Error! Reference source not found. gives an overview of the results of all fatigue experiments, with "Experiment" the unique test ID, "Spec" the specimen on which the test was carried out, "Size load" the dimensions of the load plate, "Wheel" the number of wheels, with S for a single wheel print and D for a double wheel print, *F* the upper load applied in the fatigue test, F/P_{max} the ratio of applied load in the fatigue test to the failure load P_{max} in the corresponding static test, *N* the number of cycles to failure or for the corresponding load level, "Age" the age of the specimen and testing, and $f_{cm,cube}$ the cube concrete compressive strength at the age of testing. For the fatigue tests with a large number of cycles, taking many days, two values are given for $f_{cm,cube}$: the strength at the first and the strength at the last day of testing.

3.2 Analysis of parameters

The first parameter that was varied is the distance between the ducts. The centre-to-centre spacing of 400 mm corresponds to the most unfavourable situation encountered in the bridge after which the setup is modelled. The effect of the duct spacing was analysed in the static and fatigue tests. The conclusion from the static tests was that the influence of the duct spacing on the failure load is limited. For the fatigue tests, experiment BB26 (see **Error! Reference source not found.**) with a duct spacing of 300 mm can be compared to experiment BB 28 (see **Error! Reference source not found.**) with a duct spacing of 400 mm. The results seem to indicate that the large duct spacing is not the most unfavourable situation. Additional experiments are necessary to further analyse the effect of this parameter, given the large scatter inherent to fatigue testing.

The effect of the sequence of load levels was studied in the first and second series. In the first series, the results of BB32 (higher load level followed by lower load level) and BB28 (lower load level followed by higher load level) can be compared, see **Error! Reference source not found.**. The number of cycles to failure in BB32 was significantly smaller than in BB28, which raised concerns about the effect of a small number of heavily overloaded trucks on the fatigue life of existing slab-between girder bridges. Therefore, this parameter was studied further in the second series of experiments. In the second series, both low-to-high variable amplitude fatigue loading as well as high-to-low variable amplitude fatigue loading was used. As can be seen in **Error! Reference source not found.**, the difference in results for low-to-high and high-to-low loading is negligible.

The effect of the number of wheel loads is studied as well. The conclusion of the static tests on specimens 1 and 2 was that the maximum load for the case with a double wheel print is on average 1.56 times the maximum load for the case with a single wheel print. The failure mode for the case with a double wheel print was punching of one of the two wheels through the slab. The results of the first series of fatigue tests indicates a similar trend for the difference between the double and single wheel print. With the additional test results of the second series, it was concluded that there is no significant difference in fatigue behaviour between single and double wheel prints. Further analyses of the experimental results are given in [17, 18].

3.3 Resulting *S-N* curve

From the reported experiments, a Wöhler curve (S-N curve, with S the load ratio F/Pmax and N the number of cycles to failure) is developed for the assessment of slab-between-girder bridges. As shown in Table 3, in a number of experiments variable amplitude loading was used when after a large number of cycles failure did not occur for a given load level. These experiments are accounted for as follows: say that an experiment is done with N1 cycles at load level F1, N2 cycles at F2, and N3 at F3, with load levels F1 < F2 < F3. It is then conservative to say that the deck can withstand at least N1 + N2 + N3 cycles at F1, N2 + N3 cycles at F2, and N3 cycles at F3. As such, this one experiment results in three datapoints for the S-N curve. From the first series of experiments, 16

datapoints are gathered. From the second series of experiments, 28 datapoints are gathered. From the combination of these experiments, see Figure 3, the following S-N relation is derived:

$$S = -0.062 \log N + 0.969 \quad (1)$$

The resulting S-N curve shows that the fatigue strength for 1 million cycles is 60% of the static strength. This ratio is similar to the reduction of the compressive strength due to cycles of loading (Lantsoght et al. 2015, Lantsoght et al. 2016). If the reduction due to fatigue would be larger than the reduction of the strength of the materials, then these experiments would be giving an indication that compressive membrane action is lost as a result of progressive cracking in fatigue testing. However, these experiments show the contrary: compressive membrane action remains a load-carrying mechanism for thin transversely prestressed concrete slabs subjected to cycles of loading. Under cycles of live loading, compressive membrane action enhances the capacity of thin transversely prestressed concrete decks, and this positive effect can be taken into account for the assessment of existing slab-between-girder bridges.

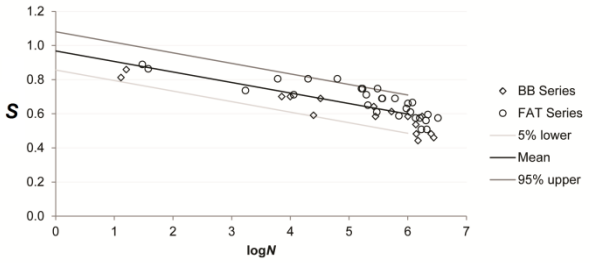

Figure 3. S-N relationship for all experiments

4 Summary

Upon assessment, the thin decks of existing slab-between-girder bridges in The Netherlands are found to have an insufficient punching shear capacity. However, the code provisions used for the assessment do not take into account the capacity-enhancing effect of compressive membrane action. Static tests on a 1:2 scale slab-between-girder bridge in the laboratory showed that the ultimate capacity of the decks is on average 2.3 times larger than the capacity calculated with the code provisions.

Fatigue loading results in progressive cracking and can result in strain increases. To use the capacity-enhancing effect of compressive membrane action, it needs to be shown that compressive membrane action does not break down under cycles of loading. For this purpose, two series of experiments were carried out. On the original specimen, two fatigue tests and two tests with a cyclic loading protocol of three cycles per load level were done, followed by five fatigue tests on a newly cast deck between the existing girders. In the second series of tests, a new specimen was built for which the top flange of the girders and the deck was cast monolithically, resulting in ten more fatigue tests.

The parameters studied in these experiments are the effect of the duct spacing, the effect of multiple wheel loading, and the effect of variable amplitude fatigue loading. We find no conclusive results regarding the duct spacing. The fatigue life of a deck under a single wheel print is similar to the fatigue life of a deck under a double wheel print. Miner's rule is found to be valid for variable amplitude fatigue loading.

Based on all experiments, the *S-N* curve for thin transversely prestressed concrete decks is developed. The fatigue strength at 1 million cycles is 60% of the static strength, which corresponds to the reduction in concrete compressive strength. As such, it is proven experimentally that compressive membrane action remains a load-carrying mechanism under cycles of loading.

5 Acknowledgments

The authors wish to express their gratitude and sincere appreciation to the Dutch Ministry of Infrastructure and the Environment (Rijkswaterstaat) for financing this research work. We are deeply indebted to our colleague Albert Bosman for his work in the laboratory and the meticulous reporting of the experiments. We'd also like to thank our former colleagues Sana Amir and Patrick van Hemert for their contributions to the beginning of this research project.

6 References

1. Code Committee 351001, *NEN 6720 Technical Foundations for Building Codes,*

Concrete provisions TGB 1990 - Structural requirements and calculation methods (VBC 1995) (in Dutch). 1995, Delft, The Netherlands: Civil engineering center for research and regulation, Dutch Normalization Institute,. 245.

2. CEN, *Eurocode 2: Design of Concrete Structures - Part 1-1 General Rules and Rules for Buildings. NEN-EN 1992-1-1:2005*. 2005, Comité Européen de Normalisation: Brussels, Belgium. p. 229.
3. Lantsoght, E.O.L., et al., *Recommendations for the Shear Assessment of Reinforced Concrete Slab Bridges from Experiments* Structural Engineering International, 2013. **23**(4): p. 418-426.
4. Amir, S., et al., *Experiments on Punching Shear Behavior of Prestressed Concrete Bridge Decks.* Aci Structural Journal, 2016. **113**(3): p. 627-636.
5. Collings, D. and J. Sagaseta, *A review of arching and compressive membrane action in concrete bridges.* Institution of Civil Engineers – Bridge Engineering, 2015. **169**(4): p. 271-284.
6. Kuang, J.S. and C.T. Morley, *A Plasticity Model for Punching Shear of Laterally Restrained Slabs with Compressive Membrane Action.* International Journal of Mechanical Sciences, 1993. **35**(5): p. 371-385.
7. Tong, P.Y. and B. de V. Batchelor, *Compressive membrane enhancement in two-way bridge slabs.* SP 30-12, 1972: p. 271-286.
8. Amir, S., *Compressive Membrane Action in Prestressed Concrete Deck Slabs*. 2014, Delft University of Technology. p. 317.
9. Zeng, D., et al., *Exploratory Experimental Study on Fatigue Prestress Loss of Prestressed Concrete Beams.* Journal of Highway and Transportation Research and Development (English Edition), 2014. **8**(2): p. 37-41.
10. Harajli, M.H. and A.E. Naaman, *Static and Fatigue Tests on Partially Prestressed Beams.* Journal of Structural Engineering, 1985. **111**(7): p. 1602-1618.
11. Naaman, A.E. and M. Founas, *Partially Prestressed Beams under Random-Amplitude Fatigue Loading.* Journal of Structural Engineering, 1991. **117**(12): p. 3742-3761.
12. El Shahawi, M. and B. de V. Batchelor, *Fatigue of Partially Prestressed Concrete.* Journal of Structural Engineering, 1986. **112**(3): p. 524-537.
13. Koekkoek, R.T. and C. van der Veen, *Measurement Report Fatigue Tests on Slabs Cast In-Between Prestressed Concrete Beams*. 2017. p. 196.
14. Koekkoek, R.T. and C. van der Veen, *Analysis of Test Results for Fatigue Tests on Slabs Cast In-Between Prestressed Concrete Beams*. 2017. p. 21.
15. van der Veen , C. and A. Bosman, *Fatigue strength of prestressed cast-in-between deck panels (in Dutch)*. 2014. p. 65.
16. CEN, *Eurocode 1: Actions on structures - Part 2: Traffic loads on bridges, NEN-EN 1991-2:2003*. 2003, Comité Européen de Normalisation: Brussels, Belgium. p. 168.
17. Lantsoght, E.O.L., et al., *Punching capacity of prestressed concrete bridge decks under fatigue.* ACI Structural Journal, 2019. **116**(4): p. 209-2018.
18. Lantsoght, E.O.L., et al., *Capacity of prestressed concrete bridge decks under fatigue loading*, in *fib symposium 2019*. 2019: Cracow, Poland.